Two-beam energy exchange in a hybrid photorefractive-flexoelectric liquid-crystal cell

V. Yu. Reshetnyak,[1] I. P. Pinkevych,[1] G. Cook,[2,3,*] D. R. Evans,[2] and T. J. Sluckin[4]
[1]*Physics Faculty, National Taras Shevchenko University of Kyiv, Volodymyrs'ka Street 64, Kyiv 01601, Ukraine*
[2]*Air Force Research Laboratory, Materials and Manufacturing Directorate, Wright-Patterson Air Force Base, Ohio 45433, USA*
[3]*Universal Technology Corporation, 1270 N. Fairfield Road, Dayton, Ohio 45432, USA*
[4]*School of Mathematics, University of Southampton, Highfield, Southampton SO17 1BJ, United Kingdom*
(Received 5 August 2009; published 17 March 2010)

We develop a semiquantitative theory to describe the experimentally observed energy gain when two light beams intersect in hybrid organic-inorganic photorefractives. These systems consist of a nematic liquid-crystal (LC) layer placed between two photorefractive windows. A periodic space-charge field is induced by the interfering light beams in the photorefractive windows. The field penetrates into the LC, interacting with the nematic director and giving rise to a diffraction grating. LC flexoelectricity is the principal physical mechanism driving the grating structure. Each light beam diffracts from the induced grating, leading to an apparent energy gain and loss within each beam. The LC optics is described in the Bragg regime. In the theory the exponential gain coefficient is a product of a beam interference term, a flexoelectricity term and a space-charge term. The theory has been compared with results of an experimental study on hybrid cells filled with the LC mixture TL 205. Experimentally the energy gain is maximal at much lower grating wave numbers than is predicted by naïve theory. However, if the director reorientation is cubic rather than linear in the space-charge field term, then good agreement between theory and experiment can be achieved using only a single fitting parameter. We provide a semiquantitative argument to justify this nonlinearity in terms of electric-field-induced local phase separation between different components of the liquid crystal.

DOI: 10.1103/PhysRevE.81.031705 PACS number(s): 42.70.Df, 42.79.Kr, 42.65.Hw

I. INTRODUCTION

In solid inorganic crystals energy transfer between incident light beams in a two-wave mixing geometry due to the photorefractive effect is well known [1]. In these systems a small relative refractive index modulation of order $\sim 10^{-4}$ can cause intensity gain coefficients as high as $10-100\ \mathrm{cm}^{-1}$ [2]. Significant photorefractivelike interactions have been also observed in liquid-crystal (LC) cells in recent years. Here there is a relatively high index modulation of order 0.2 caused by LC director reorientation. For these systems, very strong two-beam energy transfer between two coupled beams has been observed [3–5], with gain coefficient reaching $2890\ \mathrm{cm}^{-1}$ [4]. The physical mechanism for liquid-crystal (or so-called "organic") photorefraction is as follows. The nematic LCs are photoconductive. The diffusion constants of the photogenerated negative and positive ions differ, leading to charge separation, which in turn causes a space-charge electric field. It is this electric field which modulates the nematic director field and hence causes a modulation the (tensor) refractive index. This phenomenon is known as orientational photorefraction [6–8].

In a related set of systems, photorefractive or photoconducting layers are placed adjacent to a LC sample [9–11]. In a beam-coupling geometry, space charges are photogenerated in the photorefractive/photoconducting layers, leading, as might be expected, to space-charge electric fields. These space-charge electric fields leak into the adjacent LC, causing director modulation. These ("hybrid organic-inorganic photorefractive") systems also exhibit enhanced two-beam coupling. The gain coefficients in such systems can even reach values more than two orders of magnitude larger than those in solid inorganic photorefractive crystals. The gain coefficients in these experiments are sufficiently large that these systems are attracting interest from an applications point of view. However, it has until very recently only been possible to operate in the Raman-Nath regime, for which the sample thickness is less than the grating thickness. In this regime, coupled beams also generate multiple order diffracted beams. To minimize this effect, the angle between the pump and signal beams is restricted to less than a few degrees. Thus the effect might only be of limited technological applicability.

However, in very recent work, some of us have shown [12,13] that inorganic photorefractive crystals have a sufficiently large effective trap density to support efficient space-charge field generation necessary to reach the Bragg regime [13–15]. In this regime the sample thickness is greater than the grating thickness. In these experiments, the Bragg regime applies to the nonlinear optics both in the inorganic photorefractive layers and in the adjacent LC layers. Key features of these experiments include: (a) a maximum in the energy gain at small grating spacings $\sim(1.5-2)\mu$m and (b) a gain coefficient which can reach $600\ \mathrm{cm}^{-1}$, depending on the LC cell thickness. Even greater two-beam coupling effects have been observed in other hybrid organic-inorganic photorefractives, for which the LC is doped either by a low concentration of ferroelectric nanoparticles [16] or by chiral impurities [17]. However, in all these systems, the precise mechanisms remain unclear.

The idea that an evanescent field from a space-charge field from inside a photorefractive substrate could reorient a LC director and hence lead to grating formation was first

*Present address: Azimuth Corporation, 4134 Linden Avenue, Suite 300, Dayton, OH 45432, USA.

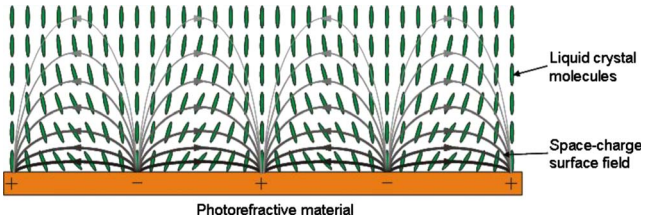

FIG. 1. (Color online) The periodic space-charge field from inside the photorefractive substrate penetrates into the liquid crystal. This reorients the liquid crystal director, allowing the cell to act as a grating.

proposed a decade ago by Tabiryan and Umeton [18]. This effect is shown in cartoon form in Fig. 1. Jones and Cook [19] used this idea to model a so-called dual photorefractive substrate device, in which a liquid-crystal slab is sandwiched between two photorefractive samples. In these papers the evanescent electric field couples with the director through (and only through) the LC static dielectric anisotropy, leading to the formation of a director grating. In these systems the LC layer is thin compared to adjacent photorefractive substrate. However, the evanescent field idea has also been applied to systems in which a very thin photoconductive PVK (poly[3-3′ (vinylcarbazole)]) layer has been attached to the liquid-crystal surface [20–22].

In this paper we make a theoretical study of our beam-coupling experiments in hybrid organic-inorganic photorefractives [13–15]. The geometry of these experiments is shown in Fig. 2. The theory uses the evanescent fields as a key idea. We note that from a technological point of view, maximal effects may require either chiral or nanoparticle impurities or both [16,17]. However, we begin with a physical picture for simpler cases which omit these complications. A sensible starting point is naïvely to apply the ideas expounded in the theoretical papers of Tabiryan and Umeton [18] and Jones and Cook [19]. But we find that doing this yields a maximal energy transfer for grating spacings of the order of the LC cell thickness. In fact this prediction is not borne out by experiment.

In the calculation presented in this paper, the flexoelectric interaction between the director and the electric field is also included. This effect has not been previously included in theoretical calculations. However, the experiments of Cook *et al.* [13] have hinted strongly that flexoelectric effects are important. We shall show that this is a more important mechanism for electric field-director coupling than the LC static dielectric anisotropy coupling discussed in Refs. [18,19].

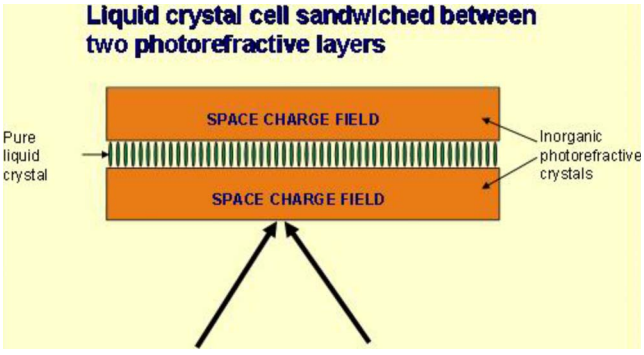

FIG. 2. (Color online) The geometry of two beam-coupling experiments in hybrid organic-inorganic photorefractives.

However, we need to include one extra new theoretical idea. We find that the results [13–15] cannot be explained consistently without including a nonlinear contribution to the magnitude of the grating as a function of optical electric field intensity. This paper includes results of an independent experimental study of two-beam energy exchange in hybrid photorefractive cells filled with the LC mixture TL 205. This experiment, which involves a third beam, has been specifically designed to pinpoint this contribution. The presence of the nonlinear term has been explicitly confirmed by this experiment. We speculate that this nonlinearity, which affects the flexoelectric coupling, might be caused by electric-field-induced component separation in a multicomponent liquid crystal. This speculation is supported by a semiquantitative calculation which gives the right order of magnitude and functional dependence on grating spacing. It is then possible to provide an excellent fit to the experimental results using only one fitting parameter.

The paper is organized as follows. In Sec. II we introduce the model, concentrating on the interfering incident light beams and the space-charge field in the photorefractive substrates. We also define the crucial quantities associated with gain. In Sec. III we discuss the evanescent space-charge field in the LC, derive equations for the LC director subject to this electric field, and then solve them. In Sec. IV we discuss light propagation in the LC, starting with expressions for the dielectric tensor, going on to derive equations for the two coupled light modes, and finally deriving expressions for the exponential gain coefficient in the LC cell. In Sec. V, we make comparisons with experimental results and find that the basic linear theory which we have developed fails to account for the experiments. We develop an alternative nonlinear picture, compare this picture with experiments, and report on experiments which corroborate our alternative phenomenological model. In Sec. VI we discuss the microscopic status of the phenomenological model we have introduced and give further reasons for believing that the picture we have developed is correct. We also present some brief further conclusions.

II. MODEL

The experiment consists of a hybrid cell consisting of flexoelectric nematic LC placed between two plane-parallel transparent photorefractive layers. The LC is bounded by the planes $z=-L/2$ and $z=L/2$. The hybrid cell is illuminated by two intersecting coupled polarized coherent light beams $\mathbf{E}_1 = A_1(z)\mathbf{e}_1 \exp(i\mathbf{k}_1\cdot\boldsymbol{r}-i\omega t)$ and $\mathbf{E}_2=A_2(z)\mathbf{e}_2 \exp(i\mathbf{k}_2\cdot\boldsymbol{r}-i\omega t)$. In the context of propagation in the LC, these beams are extraordinary waves. The nonlinear properties of both media require that $A_1(z)$ and $A_2(z)$ not be constant but change as a function of position, as energy exchange takes place between the beams. The bisector of the beams is directed along the z axis, the wave vectors $\mathbf{k}_1$ and $\mathbf{k}_2$ and the polarization vectors

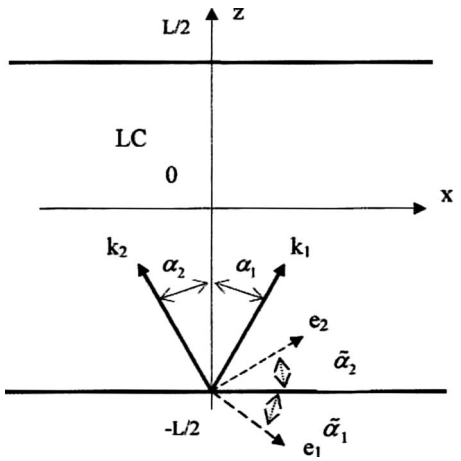

FIG. 3. Experimental set-up, showing light beams incident from photorefractive medium, together with associated wave- and polarization vectors. The quantities $k_1, \alpha_{1,2}, \tilde{\alpha}_{1,2}, \mathbf{e}_{1,2}$ are defined in the text

$\mathbf{e}_1$ and $\mathbf{e}_2$ of the beams, and the liquid-crystal directors all lie in the xz plane. The experimental setup is shown in Fig. 3.

Energy transfer takes place between beams within the photorefractive medium. This is well-understood phenomenon. Energy transfer also takes place within the liquid crystal, and much of this paper will concentrate specifically on this region. The beams form a light intensity interference pattern

$$I(z) = (I_1 + I_2)\left\{1 + \frac{1}{2}[m(z)\ \exp(iqx) + \text{c.c.}]\right\}, \qquad (1)$$

where the modulation parameter $m(z) = 2\ \cos(2\delta)A_1(z)A_2^*(z)/(I_1+I_2)$, 2δ is the angle between the two incident beams in the photorefractive medium, $I_1 = A_1A_1^*$ and $I_2 = A_2A_2^*$ are the intensities of the incident beams, and $q = k_{1x} - k_{2x} = 2k\ \sin\ \delta \approx 2k\delta$ is the wave number of intensity pattern [[23], p. 84].

Within the photorefractive layers the light intensity pattern [Eq. (1)] induces a space charge. The fundamental Fourier component of the space-charge density is modulated along the x axis with period equal to $2\pi/q$ and creates a space-charge electric field $\frac{1}{2}\boldsymbol{E}_{sc}(q,z)\exp(iqx) + \text{c.c.}$, where $\boldsymbol{E}_{sc}(q,z) = \mathbf{E}_{0sc}(q)m(z)$ depends on the physical properties and geometry of the photorefractive material.

In an infinite photorefractive medium $\boldsymbol{E}_{0sc}(q)$ is parallel to the x-axis (i.e., the grating vector). For a diffusion-dominated space-charge field, $\boldsymbol{E}_{0sc}(q)$ takes the following form [[23], p. 89]:

$$E_{0sc}(q) = \frac{iE_d}{1 + \dfrac{E_d}{E_q}}, \quad E_d = q\frac{k_bT}{e}, \quad E_q = \left(1 - \frac{N_a}{N_d}\right)\frac{eN_a}{\varepsilon_0\varepsilon_{Ph}q}, \qquad (2)$$

where E_d is the diffusion field, E_q is the so-called saturation field, N_a and N_d are, respectively, the acceptor and donor impurity densities, ε_{Ph} is the dielectric permittivity of photorefractive material, and e is the electron charge. The relation $\mathbf{E} = -\nabla\Phi$ yields the following approximate form for the total electric potential $\Phi(x,z)$ in the photorefractive medium:

$$\Phi(x,z) = \Phi_0 + \frac{1}{2}[i\tilde{\Phi}(z)\exp(iqx) + \text{c.c.}] \qquad (3)$$

where Φ_0 is an arbitrary constant (which may be taken to be zero), and

$$\tilde{\Phi}(z) = \frac{E_{0sc}(q)}{q}m(z). \qquad (4)$$

The photorefractive media are not infinite but semi-infinite. Thin polymer layers between the liquid crystal and the photorefractive media play the dual roles of orientating layers for the liquid crystal and charge caps preventing the space charges in the photorefractive media from escaping. The confinement of the charges causes the expressions for the fields [Eq. (2)] to hold approximately in the photorefractive media right up to the liquid-crystal boundaries. The solution for the electric fields in the photorefractive media and the liquid crystal is actually a complex coupled problem. However, if we suppose that Eq. (2) remains true at the liquid-crystal-photorefractive media boundaries, the electric field problems in the two media separate, with Eqs. (2) now acting as boundary conditions for the electric potential within the liquid crystal.

In much of this paper we shall be specifically interested in the progress of the coupled waves through the liquid-crystal medium. We can calculate the amplitudes of the beams as they are incident on the liquid-crystal slab using the well-known theory [23] of beam coupling in photorefractive material alone. We can thus define the quantities

$$B_1 = A_1\left(-\frac{L}{2}\right), \quad B_2 = A_2\left(-\frac{L}{2}\right). \qquad (5)$$

The specific goal of this paper is to calculate the analogous quantities for the beams as they exit the liquid-crystal slab. We denote these by

$$C_1 = A_1\left(\frac{L}{2}\right), \quad C_2 = A_2\left(\frac{L}{2}\right). \qquad (6)$$

An important intermediate quantity in the calculation is the modulation parameter $m(z)$. We consider only the case when the intensity of one light beam (signal) is much less than the intensity of another light beam (pump), namely, $I_1 \ll I_2$. In this case the values of the modulation parameter associated with the beams as they enter and exit the liquid-crystal slab are described by the following expressions:

$$m_1 = m\left(-\frac{L}{2}\right) = 2\ \cos(2\delta)\frac{B_1}{B_2}, \quad m_2 = m\left(\frac{L}{2}\right) = 2\ \cos(2\delta)\frac{C_1}{C_2}. \qquad (7)$$

The two beams under consideration are conventionally regarded as a signal beam, containing relevant information, and a pump beam which conveys no information but provides energy which is transferred into the signal beam. In this paper the signal beam is denoted by the amplitude $A_1(z)$, and the pump beam is denoted by the amplitude $A_2(z)$. The

nonlinear properties of the liquid-crystal layer are defined by the transmission operator M, where

$$\mathbf{C}=\mathbf{MB}, \quad \mathbf{C}=\begin{bmatrix} C_1 \\ C_2 \end{bmatrix}, \quad \mathbf{B}=\begin{bmatrix} B_1 \\ B_2 \end{bmatrix}, \quad \mathbf{M}=\begin{bmatrix} M_{11} & M_{12} \\ M_{21} & M_{22} \end{bmatrix}. \tag{8}$$

The degree of transfer from the pump into the signal beams is conventionally described in terms of a total signal gain $G=M_{11}$. This can be translated into an effective gain coefficient (or sometimes *exponential gain coefficient*) g, the gain per unit length of the signal beam, where

$$g=\frac{1}{L}\ln|G|. \tag{9}$$

The physical mechanism for the nonlinear optical activity within the liquid-crystal slab has been described in outline in the introduction. The space-charge fields due to the wave interference in the photorefractive media leak into the liquid-crystal slab. These fields reorient the liquid-crystal director. This in turn sets up a periodic grating which causes energy exchange between the beams.

One may ask why it is worth putting in the liquid-crystal layer when the photorefractive layers already create a nonlinear optical medium. In fact the effect of the space charges is to create electric fields which reorient the director *outside* the photorefractive region. The director is extremely sensitive even to weak fields. Thus, in some sense, the presence of the liquid crystal allows the experimenter to use the space-charge fields to create beam exchange even outside the specifically photorefractive regions. If the liquid-crystal slab is too thin, then these fields are not being used optimally. If it is too thick, then there will be part of the liquid-crystal slab in which the evanescent fields have decayed too far. From the point of view of optical gain, when this is the case, some liquid crystal is being wasted.

The calculation presented in this paper contains two self-consistent steps, one of which cannot be avoided even approximately. The gain depends on the transmission operator **M**. The operator **M** depends on the dielectric profile within the slab, which in turn depends on the director profile. The director reorientation depends on the electric field. The electric field depends weakly on the director. This involves a self-consistent step, but one which can be omitted in a preliminary calculation without great cost. In this paper we adopt this strategy.

The electric field inside the liquid crystal also depends crucially on the boundary conditions for the electric potential. We explain above our procedure for decoupling the electric problem into a bulk photorefraction and a liquid-crystal surface problem. This simplifies the problem somewhat. But the surface problem nevertheless requires knowledge of the electric potential where the beams exit the liquid-crystal slab. But this electric potential depends on space charge, hence on the modulation parameter m_2, and hence on the transmission operator **M**. This self-consistency step is unavoidable although in practice the gain G over the liquid-crystal slab is sufficiently close to unity that the self-consistency of the calculation is not so important.

We have now described the formal stages required in carrying out the calculation. The first step, to be discussed in Sec. III, involves a calculation of the director, and hence the dielectric profile. The next step, to be discussed in Sec. IV, involves the derivation of the transmission properties of the liquid-crystal layer.

III. DIRECTOR PROPERTIES

A. Photorefractive electric field in liquid crystal

We now discuss the penetration into the LC of the space-charge electric field in the photorefractive media. The electric field obeys the Poisson equation

$$\boldsymbol{\nabla}\cdot(\varepsilon_0\hat{\tilde{\varepsilon}}\cdot\mathbf{E}+\mathbf{P}_f)=0, \tag{10}$$

where $\tilde{\varepsilon}_{ij}=\tilde{\varepsilon}_\perp\delta_{ij}+\tilde{\varepsilon}_a n_i n_j$ is the low-frequency dielectric permittivity of the LC, n_i are the components of the director **n**, $\tilde{\varepsilon}_a=\tilde{\varepsilon}_\parallel-\tilde{\varepsilon}_\perp$ is the dielectric anisotropy, $\tilde{\varepsilon}_\parallel$ and $\tilde{\varepsilon}_\perp$ are the components of the dielectric tensor along and perpendicular to the director. The flexopolarization $\mathbf{P}_f$ is defined by the expression [24,25]:

$$\mathbf{P}_f=e_{11}\mathbf{n}\,\boldsymbol{\nabla}\cdot\mathbf{n}+e_{33}(\boldsymbol{\nabla}\times\mathbf{n})\times\mathbf{n}, \tag{11}$$

where e_{11} and e_{33} are the flexoelectric coefficients.

We note that the director field $\mathbf{n}(z)$ responds to the electric field defined in Eq. (10) and that technically it is necessary to solve Eqs. (10) and (11) self-consistently with equations for the director. However, we will consider only small deviations of the director in response to the electric field. In this case we can neglect the feedback of the director response on the electric field in the photorefractive medium. Detailed calculations (not included here) demonstrate that the neglected terms give negligibly small contribution to the gain. Thus we can ignore Eq. (11) at this stage of the calculation.

To solve Eq. (10) inside the liquid crystal, we use the relation $\mathbf{E}(x,z)=-\boldsymbol{\nabla}\Phi_{LC}(x,z)$ and seek solutions for the electric potential Φ_{LC} in the form

$$\Phi_{LC}=\Phi_0(z)+\frac{1}{2}[i\Phi(z)\exp(iqx)+\text{c.c.}]. \tag{12}$$

Combining Eqs. (10) and (12) yields

$$\frac{\partial^2\Phi_0}{\partial z^2}=0, \tag{13}$$

$$\tilde{\varepsilon}_\perp\frac{\partial^2\Phi}{\partial z^2}-\tilde{\varepsilon}_\parallel q^2\Phi=0. \tag{14}$$

Using Eq. (4), the boundary conditions for the electric potentials at the liquid-crystal boundaries $z=\mp\frac{L}{2}$ can now be written as

$$\Phi_0(z=\mp L/2)=0, \quad \Phi(z=\mp L/2)=\Phi_{1,2}, \tag{15}$$

where

$$\Phi_1=\frac{E_{0sc}(q)}{q}m_1, \quad \Phi_2=\frac{E_{0sc}(q)}{q}m_2, \tag{16}$$

and m_1, m_2 are defined in Eq. (7).

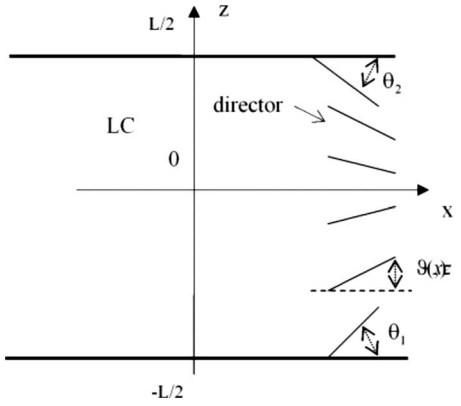

FIG. 4. Experimental set-up, showing quantities associated with the director, as discussed in text.

The solution to Eqs. (13) and (14) which satisfies boundary conditions (15) yields the following expressions for the electric field inside the LC layer:

$$E_x = E_{0x}\exp(iqx) + \text{c.c.}, \quad E_z = E_{0z}\exp(iqx) + \text{c.c.} \quad (17)$$

where

$$E_{0x} = q\left(\frac{\Phi_1+\Phi_2}{4}\frac{\cosh(\tilde{q}z)}{\cosh(\tilde{q}L/2)} + \frac{\Phi_2-\Phi_1}{4}\frac{\sinh(\tilde{q}z)}{\sinh(\tilde{q}L/2)}\right),$$

$$E_{0z} = -i\tilde{q}\left(\frac{\Phi_1+\Phi_2}{4}\frac{\sinh(\tilde{q}z)}{\cosh(\tilde{q}L/2)} + \frac{\Phi_2-\Phi_1}{4}\frac{\cosh(\tilde{q}z)}{\sinh(\tilde{q}L/2)}\right),$$

$$\tilde{q} = q\sqrt{\frac{\tilde{\varepsilon}_\parallel}{\tilde{\varepsilon}_\perp}}, \quad (18)$$

B. Director equation

As the director is confined to the xz plane, the director spatial profile in the nematic cell can be completely defined in terms of the angle $\vartheta(x,z)$ between the director and the x axis (Fig. 4),

$$\mathbf{n} = [\cos\vartheta(x,z), 0, \sin\vartheta(x,z)]. \quad (19)$$

The equilibrium director profile can now be found by minimizing the total free-energy functional of the LC cell defined by

$$F = F_{el} + F_l + F_E + F_{fl}, \quad (20)$$

subject to so-called strong anchoring conditions

$$\vartheta(x, z = -L/2) = \theta_1,$$

$$\vartheta(x, z = L/2) = \theta_2, \quad (21)$$

where θ_1 and θ_2 are the angles of the director easy axis on the planes $z = \mp\frac{L}{2}$, respectively.

We include explicitly the following contributions to the free energy: the Frank-Oseen elastic energy, with splay, twist, and bend elastic constants, respectively, K_{11}, K_{22}, K_{33},

$$F_{el} = \frac{1}{2}\int [K_{11}(\nabla\cdot\mathbf{n})^2 + K_{22}(\mathbf{n}\cdot\nabla\times\mathbf{n})^2 + K_{33}(\mathbf{n}\times\nabla\times\mathbf{n})^2]dV$$
$$= \frac{1}{2}\int \left\{K_{11}\left[\left(\frac{\partial\vartheta}{\partial z}\right)^2 + \left(\frac{\partial\vartheta}{\partial x}\right)^2\right] + (K_{33}-K_{11}) \times\left[\frac{\partial\vartheta}{\partial x}\frac{\partial\vartheta}{\partial z}\sin 2\vartheta + \left(\frac{\partial\vartheta}{\partial x}\right)^2\cos^2\vartheta + \left(\frac{\partial\vartheta}{\partial z}\right)^2\sin^2\vartheta\right]\right\}dV, \quad (22)$$

and the flexoelectric free-energy term, linear in the electric field

$$F_{fl} = -\int (\mathbf{P}_f\cdot\mathbf{E})dV$$
$$= -\int \{e_{11}(\mathbf{nE})(\nabla\cdot\mathbf{n}) + e_{33}[\mathbf{E}\cdot(\mathbf{n}\nabla)\mathbf{n}]\}dV$$
$$= \int \left\{E_x\left[\frac{e_{11}+e_{33}}{2}\sin 2\vartheta\frac{\partial\vartheta}{\partial x} - (e_{11}\cos^2\vartheta - e_{33}\sin^2\vartheta)\frac{\partial\vartheta}{\partial z}\right] + E_z\left[(e_{11}\sin^2\vartheta - e_{33}\cos^2\vartheta)\frac{\partial\vartheta}{\partial x} - \frac{e_{11}+e_{33}}{2}\sin 2\vartheta\frac{\partial\vartheta}{\partial z}\right]\right\}dV. \quad (23)$$

We shall neglect the following contributions: the anisotropic part of the electrostatic free energy, quadratic in the electric field

$$F_E = -\frac{\varepsilon_0\tilde{\varepsilon}_a}{2}\int (\mathbf{n}\cdot\mathbf{E})^2 dV$$
$$= -\frac{\varepsilon_0\tilde{\varepsilon}_a}{2}\int (\cos^2\vartheta E_x^2 + \sin^2\vartheta E_z^2 + \sin 2\vartheta E_x E_z)dV, \quad (24)$$

and the light beam-LC interaction energy, with ε_a is the anisotropy of the LC dielectric permittivity at optical frequency supposing $\varepsilon_a \ll 1$

$$F_l = -\frac{\varepsilon_0\varepsilon_a}{4}\int (\mathbf{n}\cdot\mathbf{E}_{h\nu})^2 dV. \quad (25)$$

We have neglected the dielectric anisotropy term [Eq. (24)] and have asserted that the flexoelectric term is more important. This is a key step in our calculation and is somewhat counterintuitive. In most liquid-crystal contexts, flexoelectricity may be regarded as a correction to a physical problem primarily involving energy balance between dielectric anisotropy and elasticity. We have both experimental and theoretical reasons for following this procedure.

Our cell surfaces contain significant pretilt, and the existence of the pretilt makes an important contribution to the

nonlinear optics. The pretilt has opposite signs on the top and bottom substrates, causing the whole system to lack reflection symmetry in the x direction. The nonlinear optics responds noticeably to this lack of symmetry. This implies that there is a contribution to the nonlinear optics which is linear in the space-charge field (for a quadratic term would be symmetric with respect to x). Such a contribution can only be produced by flexoelectricity.

Theoretically, we estimate the order of magnitude of the dielectric anisotropy energy [Eq. (24)]. We show that this is expected to be an order of magnitude lower than the flexoelectric energies. Neglecting dielectric anisotropy is therefore a self-consistent procedure. It is interesting to note that the flexoelectric terms are linear in the space-charge field, whereas the dielectric anisotropy terms are quadratic. The usual situation in liquid-crystal problems is that symmetry considerations require the linear terms to disappear or be very small. However, mathematically one would expect that linear terms dominate quadratic terms in expansions in small quantities, and this is in fact what happens here.

To make specific estimates of the order of magnitude of the various quantities, we note the following. Typical values of the grating period are $\Lambda=(1-5)\mu$m [13], corresponding to $q=2\pi/\Lambda\sim(10^6-10^7)\mathrm{m}^{-1}$ and elastic constant $K\sim10^{-11}$ N. This yields a LC elastic energy density of the order of $Kq^2\sim(10-10^3)\mathrm{J/m}^3$. To estimate the dc-electric field value we use the value of the photorefractive (space-charge) field in an infinite photorefractive medium. This can be taken of the order of the diffusion field, yielding $E\sim E_{0sc}\sim qk_BT/e=0.026q\approx3\times(10^4-10^5)\mathrm{V\ m}^{-1}$ [[23], p. 90]. A typical experimental static LC dielectric anisotropy in photorefractive hybrid cells is $\tilde{\varepsilon}_a\approx5$ [13]. Thus the ratio of the anisotropic part of the LC electrostatic energy density to the LC elastic energy density is of the order of $\varepsilon_0\tilde{\varepsilon}_aE^2/Kq^2\approx3\times10^{-3}$.

Estimating the flexoelectric moduli e_{11} and e_{33} presents more of a problem because these quantities are not available from the manufacturer. Edwards *et al.* [26] used a combination of macroscopic modeling and experiment to estimate these quantities for the liquid crystal E7. Cheung *et al.* [27], Stelzer *et al.* [28], and Allen and Masters [29] used simulation methods to make microscopic estimates of the flexoelectric coefficients. The upshot of this work is an estimate of $e_{11},e_{33}\sim10^{-11}$ C/m, which in turn yields a flexoelectric energy density of the order of $e_{ii}qE_{0sc}\sim(0.3-30)$ J/m^3. This implies that the ratio of the flexoelectric energy density to the elastic energy density is of the order of $e_{ii}qE_{0sc}/Kq^2\sim3\times10^{-2}$. This is one order of magnitude larger than the ratio of the anisotropic part of the electrostatic energy density to the elastic energy density and justifies *ex post facto* the inclusion of flexoelectricity in the model.

We now minimize the functional [Eq. (20)], including only terms (22) and (23). We express the director **n** explicitly in angular form using Eq. (19). We expand in small $\vartheta(x,z)$ and include terms in ϑ up to linear order. After some algebra, we obtain the following equation:

$$K_{11}\frac{\partial^2\vartheta}{\partial z^2}+K_{33}\frac{\partial^2\vartheta}{\partial x^2}+(e_{11}+e_{33})\left(\frac{\partial E_x}{\partial x}-\frac{\partial E_z}{\partial z}\right)\vartheta-e_{11}\frac{\partial E_x}{\partial z}-e_{33}\frac{\partial E_z}{\partial x}=0, \tag{26}$$

subject to the boundary conditions [Eq. (21)].

C. Director spatial profile

The angular profile of the director comes from solving Eq. (26). The director distortion $\vartheta(x,z)$ can then be represented by the following Fourier expansion:

$$\vartheta(x,z)=\theta_0(z)+[\theta(z)\exp(iqx)+\text{c.c.}], \tag{27}$$

where the zero-wave number contribution $\theta_0(z)$ is induced by the initial director pretilt at the cell surfaces, and $\theta(z)$, the amplitude of the director grating is caused by the interaction with the spatially modulated space-charge field. The optical effects will be expressed in terms of these quantities. We therefore seek to transform Eq. (26) into equations in which these are explicitly calculated.

We note that the strong anchoring conditions (21) allow us to specify Dirichlet boundary conditions both for $\theta_0(-\frac{L}{2})=\theta_1$, $\theta_0(\frac{L}{2})=\theta_2$, and for $\theta(\mp\frac{L}{2})=0$. The formal procedure involves making a transverse Fourier expansion of Eq. (26) in terms of components with wave numbers integral multiples of q. Equations for $\theta_0(z)$ and $\theta(z)$ then result if one considers separately the components associated with wave numbers 0 and q. We neglect higher-order terms in the Fourier expansion, which include higher Fourier components of the Fourier expansion given in Eq. (27).

After some algebra, we derive the following equations:

$$\frac{\partial^2\theta_0}{\partial z^2}=0, \tag{28}$$

$$K_{11}\frac{\partial^2\theta}{\partial z^2}-K_{33}q^2\theta=F(z)=-(e_{11}+e_{33})\theta_0\left(iqE_{0x}-\frac{\partial E_{0z}}{\partial z}\right)\vartheta+\left(e_{11}\frac{\partial E_{0x}}{\partial z}+iqe_{33}E_{0z}\right). \tag{29}$$

Equation (28) governs the behavior of the director in the absence of the photorefractive electric field. Equation (29) is a differential equation for $\theta(z)$, the principal Fourier component of the remaining part of director, with source terms $F(z)$ which come from the space-charge field. It is $\theta(z)$ which governs the beam-coupling properties. $F(z)$ can be divided into two groups of terms. One group contains terms proportional to the small pretilt θ_0, and one group does not contain this prefactor. A quantitatively larger contribution to $F(z)$ and hence implicitly to the director reorientation, however, come from the second group of terms which do not contain the small parameter θ_0.

The solution to Eq. (28) is

$$\theta_0(z)=s+pz,\quad s=\frac{\theta_1+\theta_2}{2},\quad p=\frac{\theta_2-\theta_1}{L}. \tag{30}$$

The solution for $\theta(z)$ can be obtained substituting expressions (18) into Eq. (30). We will take into account that in the region of interest for us, $q \approx (10^6 - 10^7)\ \mathrm{m}^{-1}$ and $L \approx (10^{-5} - 10^{-4})$ m, the inequalities $qL \gg 1$ and $\tilde{q}L \gg 1$ take place. We also suppose that $(K_{33}/K_{11})^{1/2} q \sim q$. Then, writing the solution we neglect small terms of the order of $1/qL$ and $1/\tilde{q}L$ near unity and arrive at the following form:

$$\theta(z) = \frac{1}{2}[\Phi_1 D_1(z) + \Phi_2 D_2(z)], \tag{31}$$

where

$$D_1(z) = \frac{rq\tilde{q}}{\tilde{q}^2 - q_1^2}\left\{\left[1 + \frac{i2p(\tilde{q}^2 + q^2)}{q(\tilde{q}^2 - q_1^2)}\right](e^{-q_1(z+L/2)} - e^{-\tilde{q}(z+L/2)}) - \frac{i(\tilde{q}^2 + q^2)}{q\tilde{q}}[\theta_0(z)e^{-\tilde{q}(z+L/2)} - \theta_1 e^{-q_1(z+L/2)}]\right\}, \tag{32}$$

$$D_2(z) = \frac{rq\tilde{q}}{\tilde{q}^2 - q_1^2}\left\{\left[1 + \frac{i2p(\tilde{q}^2 + q^2)}{q(\tilde{q}^2 - q_1^2)}\right](e^{\tilde{q}(z-L/2)} - e^{q_1(z-L/2)}) - \frac{i(\tilde{q}^2 + q^2)}{q\tilde{q}}[\theta_0(z)e^{\tilde{q}(z-L/2)} - \theta_2 e^{q_1(z-L/2)}]\right\}, \tag{33}$$

and where we define the quantities q_1 and r by

$$q_1 = q\left(\frac{K_{33}}{K_{11}}\right)^{1/2}, \quad r = \frac{e_{11} + e_{33}}{K_{11}}. \tag{34}$$

Finally, using the definition [Eq. (16)] for the electric potentials Φ_1 and Φ_2 and Eqs. (5)–(7) it will be useful to rewrite formula (31) for $\theta(z)$ in the form

$$\theta(z) = \frac{E_{0sc}(q)}{q}\cos(2\delta)\left[\frac{A_1(-L/2)}{A_2(-L/2)}D_1(z) + \frac{A_1(L/2)}{A_2(L/2)}D_2(z)\right]. \tag{35}$$

IV. COUPLED LIGHT MODES

In this section we investigate how the director grating obtained in the previous section influences the two beam energy exchange in the LC cell. In order to do this we calculate the liquid-crystal dielectric tensor. This will serve as input to our light propagation calculations.

A. Dielectric tensor profile

The LC dielectric tensor at an optical frequency $\varepsilon_{ij} = \varepsilon_\perp \delta_{ij} + \varepsilon_a n_i n_j$ can be written to the second order in the director angle $\vartheta(x,z)$ as

$$\hat{\varepsilon} = \begin{pmatrix} \varepsilon_\parallel - \varepsilon_a \vartheta^2(x,z) & 0 & \varepsilon_a \vartheta(x,z) \\ 0 & \varepsilon_\perp & 0 \\ \varepsilon_a \vartheta(x,z) & 0 & \varepsilon_\perp + \varepsilon_a \vartheta^2(x,z) \end{pmatrix}, \tag{36}$$

where $\varepsilon_a = \varepsilon_\parallel - \varepsilon_\perp$ and $\varepsilon_\parallel$, $\varepsilon_\perp$ are the principal values of the dielectric tensor. In Eq. (36) we left the quadratic in the director deviation angle $\vartheta(x,z)$ terms because, as we will see further, their contribution is significant. Substituting $\vartheta(x,z)$ from Eq. (27) into Eq. (36) and neglecting small terms of the second order in the angle $\theta(z)$ one can rewrite the dielectric tensor in the following way:

$$\hat{\varepsilon}(x,z) = \hat{\varepsilon}_1 + \hat{\varepsilon}_2(z) + [\hat{\varepsilon}_3(z)\exp(iqx) + \text{c.c.}], \tag{37}$$

where

$$\hat{\varepsilon}_1 = \begin{pmatrix} \varepsilon_\parallel - \varepsilon_a\theta_1^2 & 0 & \varepsilon_a\theta_1 \\ 0 & \varepsilon_\perp & 0 \\ \varepsilon_a\theta_1 & 0 & \varepsilon_\perp + \varepsilon_a\theta_1^2 \end{pmatrix}, \quad \hat{\varepsilon}_2(z) = \varepsilon_a(\theta_0(z) - \theta_1) \times \begin{pmatrix} \theta_0(z) + \theta_1 & 0 & 1 \\ 0 & 0 & 0 \\ 1 & 0 & -\theta_0(z) - \theta_1 \end{pmatrix},$$

$$\hat{\varepsilon}_3(z) = \varepsilon_a\theta(z)\begin{pmatrix} -2\theta_0(z) & 0 & 1 \\ 0 & 0 & 0 \\ 1 & 0 & 2\theta_0(z) \end{pmatrix}. \tag{38}$$

The first term in Eq. (37) corresponds to uniaxial homogeneous medium tilted at the angle θ_1 with respect to the x axis, the second term takes into account inhomogeneity of the director distribution in the LC cell due to boundary conditions at the cell planes, and the third term describes the change in the dielectric tensor due to periodic modulation of the director by the dc photorefractive electric field with period $2\pi/q$.

B. Two beam light propagation

The electric field of the light beams propagating in the liquid-crystal cell can be written in terms of the beam amplitudes $A_1(z)$ and $A_2(z)$ in the following form:

$$\mathbf{E}_{h\nu} = A_1(z)\mathbf{e}_1 \exp(i\mathbf{k}_1 \cdot \boldsymbol{r} - i\omega t) + A_2(z)\mathbf{e}_2 \exp(i\mathbf{k}_2 \cdot \mathbf{r} - i\omega t), \tag{39}$$

where (see Fig. 3) $\mathbf{e}_1 = (\cos\tilde{\alpha}_1, 0, -\sin\tilde{\alpha}_1)$, $\mathbf{e}_2 = (\cos\tilde{\alpha}_2, 0, \sin\tilde{\alpha}_2)$, $\mathbf{k}_1 = (k_1 \sin\alpha_1, 0, k_1\cos\alpha_1)$, and $\mathbf{k}_2 = (-k_2 \sin\alpha_2, 0, k_2\cos\alpha_2)$ are, respectively, the polarizations and wave vectors of the two beams. The director is only subject to small deviations from homogeneous planar orientation. In the simplest approximation, which we adopt here, we can then assume that inside the LC cell the beam polarizations and wave vectors (but not amplitudes) are unchanged, and correspond to the values taken in a homogeneous LC with dielectric tensor $\hat{\varepsilon}_1$. A more sophisticated approach, using, for example, the eikonal approximation [22], would allow the beams themselves to bend in response to the medium inhomogeneity.

The propagation constants $k_1 = \frac{\omega}{c}n_1$ and $k_2 = \frac{\omega}{c}n_2$ can be found using the well-known LC refractive index formula $n(\beta) = \sqrt{\varepsilon_\parallel \varepsilon_\perp}(\varepsilon_\perp \sin^2\beta + \varepsilon_\parallel \cos^2\beta)^{-1/2}$, where β is the angle between the light wave vector and the director. Here $n_1 = n(\beta_1)$ and $n_2 = n(\beta_2)$ where $\beta_1 = \pi/2 - \alpha_1 - \theta_1$ and $\beta_2 = \pi/2 + \alpha_2 - \theta_1$.

The light beam electric fields satisfy the usual vector wave equation [[23], p. 8]

$$[\nabla(\nabla\cdot)^{\cdot} - \nabla^2]\mathbf{E}_{h\nu} - \frac{\omega^2}{c^2}\hat{\varepsilon}(x,z)\mathbf{E}_{h\nu} = 0. \tag{40}$$

We now substitute the electric field [Eq. (39)] and the dielectric tensor $\hat{\varepsilon}(x,z)$ [Eq. (35)] into formula (40). Coupling between the waves takes place as a result of the inhomogeneous corrections to the constant dielectric tensor $\hat{\varepsilon}_1$ [[23], Chap. 2]. The electric field magnitudes $A_1(z)$ and $A_2(z)$ then vary slowly across the cell. We follow a procedure analogous to that of Jones and Cook [19], and first outlined by Kogelnik [30], who studied coupled waves in an isotropic dielectric photorefractive system in the Bragg regime. The main difference between our system and that of Jones and Cook is the existence of inhomogeneities in the z direction.

This approach is valid in the so-called Bragg regime, which holds if the Klein parameter $Q=2\pi\lambda d/n\Lambda^2$ is much greater than unity [31]. Typical values of the parameters used in our experiments are as follows: the light wavelength $\lambda=0.532$ μm, the grating spacing $\Lambda=(1-5)\mu$m, the average refractive index $n\approx 1.5$, and the hybrid cell thickness $d\approx 1$ mm. Thus we find $Q\sim 10^2-10^3$, and we expect that the Bragg regime will apply here.

We note that leading-order terms [i.e., those containing terms independent of $\theta(z)$ and $\theta_0(z)$] in this substitution must cancel, because each wave separately obeys the vector wave equation with constant dielectric tensor $\hat{\varepsilon}_1$:

$$A_1\mathbf{e}_1\nabla^2\exp(i\mathbf{k}_1\cdot\boldsymbol{r}) + \frac{\omega^2}{c^2}\hat{\varepsilon}_1 A_1\mathbf{e}_1\exp(i\mathbf{k}_1\cdot\boldsymbol{r}) = 0,$$

$$A_2\mathbf{e}_2\nabla^2\exp(i\mathbf{k}_2\cdot\boldsymbol{r}) + \frac{\omega^2}{c^2}\hat{\varepsilon}_1 A_2\mathbf{e}_2\exp(i\mathbf{k}_2\cdot\boldsymbol{r}) = 0. \tag{41}$$

After some algebra, but following the standard procedure, we now obtain from Eq. (40) the following set of coupled equations in the LC cell:

$$(\mathbf{k}_1\cdot\mathbf{e}_1)^2 A_1 + 2i[k_{1z} - e_{1z}(\mathbf{k}_1\cdot\mathbf{e}_1)]\frac{dA_1}{dz} = -k^2\mathbf{e}_1\hat{\varepsilon}_3\mathbf{e}_2\exp(i\Delta k_z z)A_2 - k^2\mathbf{e}_1\hat{\varepsilon}_2\mathbf{e}_1 A_1,$$

$$(\mathbf{k}_2\cdot\mathbf{e}_2)^2 A_2 + 2i[k_{2z} - e_{2z}(\mathbf{k}_2\cdot\mathbf{e}_2)]\frac{dA_2}{dz} = -k^2\mathbf{e}_2\hat{\varepsilon}_3^*\mathbf{e}_1\exp(-i\Delta k_z z)A_1 - k^2\mathbf{e}_2\hat{\varepsilon}_2\mathbf{e}_2 A_2, \tag{42}$$

where $\Delta k_z = k_{2z} - k_{1z}$ and $k=\frac{\omega}{c}$. The intermediate expressions in Eqs. (42) can be explicitly evaluated using Eqs. (38), yielding:

$$\mathbf{e_1}\hat{\varepsilon}_2\mathbf{e_1} = -\varepsilon_a[\theta_0(z) - \theta_1][\theta_0(z) + \theta_1 + 2\tilde{\alpha}_1],$$

$$\mathbf{e_2}\hat{\varepsilon}_2\mathbf{e_2} = -\varepsilon_a[\theta_0(z) - \theta_1][\theta_0(z) + \theta_1 - 2\tilde{\alpha}_2],$$

$$\mathbf{e_1}\hat{\varepsilon}_3\mathbf{e_2} = -2\varepsilon_a\theta_0\theta(z). \tag{43}$$

The scalar products $\mathbf{k}_1\cdot\mathbf{e}_1$ and $\mathbf{k}_2\cdot\mathbf{e}_2$ are strictly zero in isotropic media. In discussing photorefraction in anisotropic media, these terms represent a new feature, and could in principle add some new physics. But all such terms are proportional to the optical dielectric anisotropy ε_a, which is, however, a small quantity in our case. It turns out, in addition, that adding terms of $o(\varepsilon_a)$ to Eqs. (42), only add terms of $o(\varepsilon_a^2)$ to the relevant solutions. We thus feel able to neglect these terms in Eqs. (42) even though they are not strictly zero.

We recall that beam 1 is the signal and beam 2 is the pump. Furthermore, we adopt the *undepleted pump approximation*, for which the magnitude of the pump amplitude $|A_2| \gg |A_1|$ may be regarded as constant [[23], p. 152], and its phase may be taken arbitrarily as zero. In this case, Eqs. (42) reduce to

$$\frac{dA_1}{dz} = \frac{ik^2}{2k_{1z}}\mathbf{e_1}\hat{\varepsilon}_3\mathbf{e_2}\exp(i\Delta k_z z)A_2. \tag{44}$$

We also assume that the wave vectors of the light beams are symmetric with regard to the cell normal so that the angles α_1 and α_2 are equal. Then $\Delta k_z = k_{2z} - k_{1z} = \frac{\omega}{c}(n_2 - n_1)\cos\alpha_1$ is proportional to ε_a and with an accuracy to the terms of the order of $\varepsilon_a{}^2$ we can replace the exponential multiplier in Eq. (44) by unity. Finally, taking into account Eq. (43) we arrive at

$$\frac{dA_1}{dz} = is(z)A_2,$$

$$s(z) = \frac{k^2}{2k_{1z}}\mathbf{e_1}\hat{\varepsilon}_3\mathbf{e_2} = -\frac{k^2}{k_{1z}}\varepsilon_a\theta(z)\theta_0(z). \tag{45}$$

We now use this equation to investigate the optical properties of the liquid-crystal slab.

C. Exponential gain coefficient

Equations (45) can be solved, yielding the following solution in explicit form:

$$A_1(z) = A_1(-L/2) + iA_2\int_{-L/2}^{z} s(z')dz'. \tag{46}$$

We now explicitly substitute for $s(z)$ in terms of the z dependence of $\theta(z)$ from Eq. (35) in Sec. III C, yielding:

$$s(z) = -\frac{\varepsilon_a k^2}{k_{1z}}\frac{E_{0sc}(q)}{q}\frac{\cos(2\delta)}{A_2}\theta_0(z)[A_1(-L/2)D_1(z) + A_1(L/2)D_2(z)]. \tag{47}$$

The signal gain caused by the LC layer is then

$$G = \frac{A_1(L/2)}{A_1(-L/2)}, \tag{48}$$

where, from Eq. (46),

$$A_1(L/2) = A_1(-L/2) + iA_2\int_{-L/2}^{L/2} s(z)dz. \tag{49}$$

Substituting $s(z)$ from Eq. (47) into Eq. (49) yields

$$G = 1 - i\frac{\varepsilon_a k^2}{k_{1z}}\frac{E_{0sc}(q)}{q}\cos(2\delta)\int_{-L/2}^{L/2}\theta_0(z)[D_1(z) + GD_2(z)]dz. \tag{50}$$

Equation (50) yields the following expression for G:

$$G = \frac{1 + a_1}{1 - a_2}, \tag{51}$$

where

$$a_1 = -i\frac{\varepsilon_a k^2}{k_{1z}}\frac{E_{0sc}(q)}{q}\cos(2\delta)\int_{-L/2}^{L/2}\theta_0(z)D_1(z)dz,$$

$$a_2 = -i\frac{\varepsilon_a k^2}{k_{1z}}\frac{E_{0sc}(q)}{q}\cos(2\delta)\int_{-L/2}^{L/2}\theta_0(z)D_2(z)dz. \tag{52}$$

The exponential gain coefficient is given by formula

$$g = \frac{1}{L}\ln\left|\frac{1 + a_1}{1 - a_2}\right|. \tag{53}$$

We now substitute Eq. (30) for $\theta_0(z)$ and Eqs. (32) and (33) for $D_1(z)$ and, $D_2(z)$ into Eq. (52). Performing the integrations in Eq. (52) now yields

$$a_1 = \frac{\varepsilon_a r k^2 \cos(2\delta)}{k_{1z}q_1(\tilde{q} + q_1)}\left[\theta_1 + \left(1 + \frac{\tilde{q}}{q_1}\right)\frac{p}{\tilde{q}}\right]|E_{0sc}(q)|, \tag{54}$$

$$a_2 = \frac{\varepsilon_a r k^2 \cos(2\delta)}{k_{1z}q_1(\tilde{q} + q_1)}\left[-\theta_2 + \left(1 + \frac{\tilde{q}}{q_1}\right)\frac{p}{\tilde{q}}\right]|E_{0sc}(q)|. \tag{55}$$

This result is the consequence of combining standard theories for liquid crystals and photorefraction. In the next section we shall compare this result with experimental data, which demonstrate that this natural theory is deficient and that further new ideas are required.

V. EXPERIMENTS

A. Experimental parameters

We use experimental parameters from the paper by Cook *et al.* [13] and also follow their estimates for relevant material parameters. In this experiment the eutectic LC mixture TL 205 was used in photorefractive hybrid cells, with a light wavelength in air $\lambda = 0.532 \times 10^{-6}$ m, LC ordinary and extraordinary refractive indices $n_0 = 1.527$ and $n_e = 1.744$, respectively, with low-frequency dielectric constants $\tilde{\varepsilon}_{\text{II}} = 9.1$ and $\tilde{\varepsilon}_{\perp} = 4.1$. In addition, the dielectric permittivity of the photorefractive layers is given by $\varepsilon_{Ph} \approx 200$ at temperature $T = 300$ K. The liquid-crystal pretilt angle was approximately 12°, yielding $\theta_1 = 12°$, $\theta_2 = -12°$. In these estimates we assume the so-called one-elastic-constant approximation, for which $\frac{K_{33}}{K_{11}} = 1$. In addition, the quantity $\frac{k^2}{k_{1z}}\cos(2\delta)$ in Eqs. (54) and (55) includes the cosine of the small angle δ, which is proportional to the grating spacing. It is thus insensitive to the grating spacing and to a good degree of accuracy one may suppose $\frac{k^2}{k_{1z}}\cos(2\delta) = \frac{\omega}{c}\frac{\cos(2\delta)}{n_1 \cos\alpha_1} \approx 1.25\frac{\pi}{\lambda}$. In typical cases, the ratio of the acceptor to donor impurity densities is very small, $N_d \gg N_a$. Following Cook *et al.* [13], we estimate $N_a \approx 3.8 \times 10^{21}$ m^{-3}. Finally, we estimate the parameter $r = \frac{e_{11}+e_{33}}{K_{11}}$. This characteristic ratio of flexoelectric to elastic moduli is not known for TL205, but the ratio r has been measured in other liquid-crystal systems [26], and a value of 1 C m^{-1} N^{-1} may be regarded as typical. We note that in any case the value of the parameter r only influences the total magnitude of the effect, but not any other functional properties.

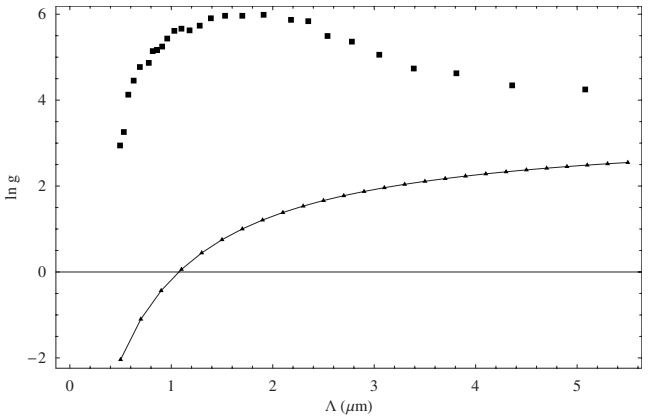

FIG. 5. Comparison of theoretical prediction based on formulas (53–55) with experimental data for liquid crystal TL 205 cell with $L = 10$ μm. Exponential gain coefficient g(in cm^{-1}) versus the grating spacing: experimental data-light boxes, theoretical prediction-curve. Note the logarithmic scale required to fit both curves in the same diagram, so poor is the agreement.

B. Comparison with theory

We first make numerical estimates of the predictions for the observed gain coefficient, using the theory of Secs. II–IV, as summarized in Eqs. (53)–(55). We compare these with the results from the work of Cook *et al.* [13]. Some extra experiments extending the range of observations have also been made especially for this paper.

In Fig. 5 we compare theoretical predictions for the exponential gain coefficient with the experiments on the eutectic LC mixture TL 205. We consider a cell of thickness 10 μm. Here, and in other figures to follow, we follow experimental convention [13] and plot the gain as a function of grating spacing $\Lambda = \frac{2\pi}{q}$ rather than as a function of the theoretically more convenient grating wave number q. The only unknown input parameter is r, the ratio of the flexoelectric to the elastic coefficient. This we suppose on rather general theoretical grounds to be of the order of unity, although our results are relatively robust with respect to changes in r.

The theory fails to account for the experiments, as can be seen rather dramatically in Fig. 5. The experimental effect is much larger than that predicted effect and occurs at lower values of the grating spacing. In fact, the disagreements are both quantitative and qualitative. The theory predicts a $g(\Lambda)$ dependence which is low at low Λ, increases approximately as Λ^2, further increases toward at a maximum $g_{\max}$ at some Λ_m, and finally decreases at high Λ. This much is in common

with the experiments. However, the theoretical value of Λ_m is of the order of 10 μm, whereas the experimental value is ~ 2 μm. Furthermore the theoretical value of $g_{\max}$ is of the order of 15, whereas the experimental value is closer to 400.

Further discrepancies between theory and experiment include the following:

(a) The experimental value of $\Lambda_m \approx 1.7$ μm is rather insensitive to cell thickness L, whereas the naïve theory seems to predict $\Lambda_m \sim L$.

(b) By contrast the experimental value of $g_{\max}$ does strongly depend on cell thickness L, whereas the theory predicts $g_{\max} \sim 10$ cm^{-1} to be insensitive to changes in L.

(c) If it is required to remedy the value of $g_{\max}$, then a wholly implausible value of $r=30$ is needed. Furthermore, $r=30$ predicts a value of Λ_m incorrect by a factor of about 5, so this fix is wholly insufficient.

Finally we note that the theory appears to predict negative $g(\Lambda)$ in the high Λ regime, again in disagreement with experiment, which seems to exhibit a point of inflection. Here, however, the theory is outside its region of validity. Roughly speaking, we might have expected the theory to be valid so long as $qL \gg 1$, where q is the grating wave number. This is equivalent to the condition $\Lambda \ll \frac{L}{2\pi}$; the approximation fails at high grating spacings.

C. Nonlinear theory

In this section we discuss the failure of the linear theory to explain the experiments and search for an alternative explanation. We first restate the result [Eq. (53)] for the gain coefficient in a slightly different language:

$$g(q,L) \approx \frac{a_1 + a_2}{L} = rI(q)H_{fl}(q)E_{0sc}(q), \tag{56}$$

where $I(q)$ is a factor which is due only to the interference between the beams, $H_{fl}(q)$ is a factor which comes from flexoelectricity, $E_{0sc}(q)$ is the space-charge field, and r is a dimensionless ratio depending on the elastic constants. The important point is that the formula for the gain factor can be separated into a product of these three factors, each of which is due to a different physical process, and that all three physical processes contribute to the full physical phenomenon. The absolute magnitude of the phenomenon is governed by the dimensionless parameter r. If the theory were correct, it might in principle be regarded as an independent measurement of r, but in any event it must be regarded as a fitting parameter for comparison with experiments.

As formula (56) has failed to reproduce the experiments, we now pose the question as to which parts of the calculation are least reliable and thus how we may make further progress. We consider the three contributions in turn:

(a) Beam interference. There are many experiments on photorefraction in orthodox photorefractive systems, for which terms such as $I(q)$ act as a driving force. These photorefractive systems are well-described by theory [23], and it seems that this part of the theory is well-founded.

(b) Flexoelectricity. Strictly speaking this term arises because of a balance between nematic flexoelectricity and elasticity. We have given an order of magnitude argument to justify our neglect of the competing dielectric anisotropy term. The key piece of experimental evidence that flexoelectricity plays an important role is the fact that cells with oppositely tilted boundaries (in which the LC in the cell is subject an intrinsic elastic bend) exhibit a much larger beam-coupling effect than cells with similar boundaries tilted in the same way.

(c) Space-charge field. We know that the space-charge field is calculated correctly, again because we are able to describe beam coupling in the bulk photorefractive systems. However, our approximation has decoupled the photorefractive and liquid-crystal systems; the bulk photorefractive system acted as a surface driving force for the liquid crystal. It seems inconceivable that the space-charge field in the bulk inorganic photorefractive far from the liquid crystal is not in some sense the ultimate driving force for the electric field effects in the liquid crystal. However, it is possible that the decoupling approximation we have adopted is not correct. It is also possible that some other physical processes couple the bulk photorefractive space-charge field to the liquid-crystal flexoelectricity. We shall discuss below some speculations as to how this might work. We propose to replace Eq. (56) by a phenomenological alternative formulation, which retain all the physics which seems most certain, but yet allows some different grating wavelength dependence of the beam-coupling gain coefficient. Thus we propose

$$g(q,L) \approx \frac{a_1 + a_2}{L} = rI(q)H_{fl}(q)F[E_{0sc}(q)], \tag{57}$$

where the function $F(w)$ is a phenomenological function to be determined. The most plausible form for $F(w)$ merely corrects the linear form $F(w) \sim w$ by a cubic correction. We thus suggest the following form:

$$F(w) = w[1 + \mu(L,q)w^2], \tag{58}$$

where the cubic correction term is dependent on the thickness of the liquid-crystal layer L and on the grating wave vector.

We thus replace Eq. (56) by the modified prediction:

$$g(q,L) \approx \frac{a_1 + a_2}{L} = rI(q)H_{fl}(q)[E_{0sc}(q) + \mu(q,L)\{E_{0sc}(q)\}^3]. \tag{59a}$$

A detailed examination of the q-dependence of Eq. (59a) at constant L, shows that in the high q (and hence low grating spacing Λ) regime, $\mu(q,L) \approx \mu(L)q^2$, where $\mu(L)$ is a function only of cell thickness L,

$$g(q,L) \approx \frac{a_1 + a_2}{L} = rI(q)H_{fl}(q)[E_{0sc}(q) + \mu(L)q^2\{E_{0sc}(q)\}^3]. \tag{59b}$$

This form now permits explicit comparison with the experimental results.

In Eq. (59b), we find that the cubic $\{E_{0sc}(q)\}^3$ term dominates to the extent that the linear $E_{0sc}(q)$ term can effectively be neglected. In Fig. 6 we compare expression (59b) with the experimental Λ dependence of $g(q,L)$ $(\Lambda = \frac{2\pi}{q})$ for a number

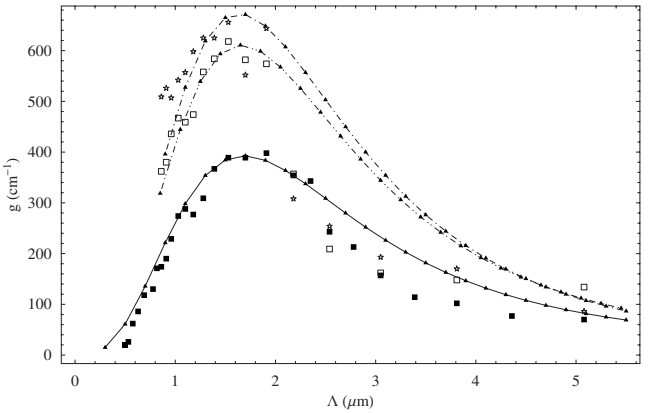

FIG. 6. Theoretical fit for the gain coefficient $g(\Lambda, L)$ compared to experimental data for liquid crystal TL 205 cells of different thickness: $L(\mu\text{m})=5.7$—stars, 7.1–light boxes, 10–black boxes.

of different values of L. In Sec. V D below we discuss experimental evidence, presented in this paper, that the particular form $\{E_{0sc}(q)\}^3$ is the correct parametrization.

The low Λ regime is fitted (and hence necessarily correct). The general features of the experimental and theoretical curves are similar. There is a maximum in $g(q,L)$ as a function of Λ. The high Λ regime is not quantitatively accurate but is nevertheless qualitatively correct. The quantity $\mu(L)\approx 2\times 10^{-21}$ in SI units, and is relatively insensitive to cell thickness L over the range $L=5-10$ μm, although we find that for $L=20$ μm, $\mu(L)\approx 10^{-21}$. Key features of the experimental results which are well-described by this parameterization, but for which the naïve theory of Secs. II–IV fails to account, are (a) the constancy of $\Lambda_m(L)\approx 1.7$ μm and (b) the magnitude of $g_{\max}(L)$. In Fig. 7, we compare theory and experiment for these quantities.

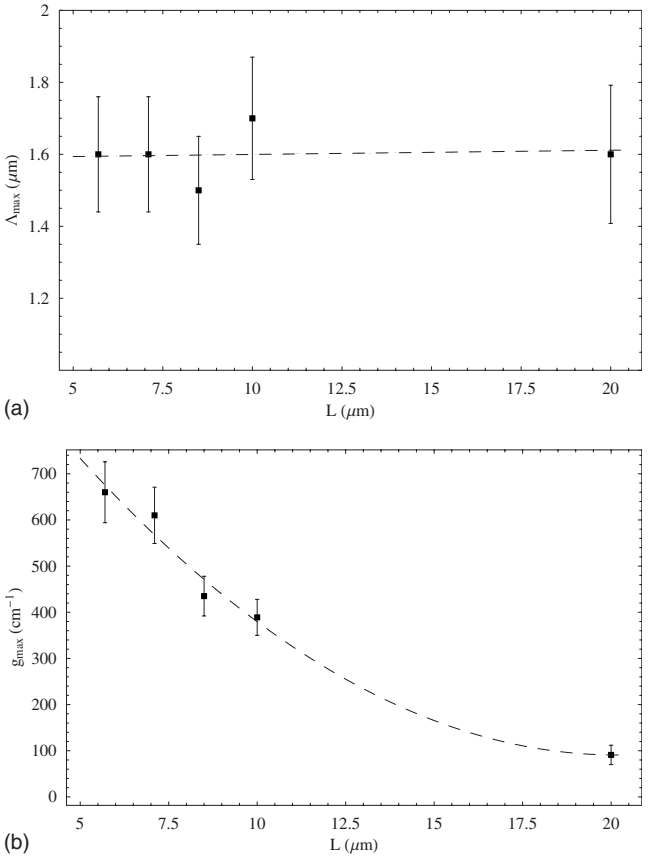

FIG. 7. Comparison of theory and experiment for different thickness L: (a) Grating spacing $\Lambda_{\max}$ at which gain is maximal. (b) Maximal gain coefficient $g_{\max}$. In each case, light boxes correspond to experiment, and stars to the theory. Note that parameters for the theory for each L have been determined by fitting at high Λ. Liquid crystal: TL 205.

D. Three beam gain experiment

We have found in the previous subsection that the most plausible explanation of the photorefractive beam-coupling data in the liquid-crystal layer requires a strong contribution to the amplitude of this effect proportional to the cube of the bulk photorefractive space-charge field in the inorganic layer. In this section we present extra experimental evidence that this cubic contribution is indeed real.

The experiment involves a third He-Ne laser beam incident on the hybrid cell. This beam possesses a different frequency from the two primary interfering beams and hence does not interfere directly with the beams which write the diffraction grating. However, the third beam does affect the magnitude of the bulk space-charge field $E_{0sc}(q)$ [see Eq. (59b)].

The experiment infers indirectly the change in $E_{0sc}(q)$ when the third beam is introduced. It does this by performing comparing gain measurements through the total sample but with the "liquid-crystal" cell filled an inert substance (in our case, oil) rather than liquid crystal. The total gain in the system, now including the liquid-crystal cell, now allows a calculation of a value of g. By comparing the gain in the presence of the third beam to that which occurs without the third beam, it is then possible directly and independently to measure the influence of the bulk space-charge field on the beam coupling.

Figure 8 shows the experimental arrangement used to introduce the third He-Ne laser beam. A continuous wave 532 nm laser generated the pump and signal beams which were p polarized. The grating spacing was controlled by adjusting the external angle between the pump and signal beams, θ, and the grating spacing, Λ, was given by $\Lambda=\lambda/2\sin(\theta/2)$. A 10 mW pump beam was used for the experiment while the incident signal beam was attenuated to 7 μW to ensure the

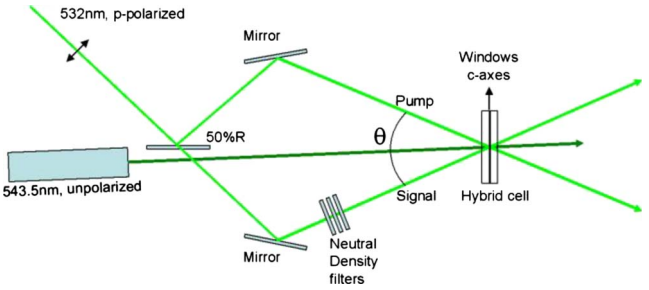

FIG. 8. (Color online) Three-beam experimental arrangement.

gain measurements were carried out in the small signal regime. The Gaussian intensity pump and signal beam spot diameters were both approximately 2.8 mm at the $1/e^2$ intensity level. An unpolarized He-Ne laser operating at 543.5 nm was used to provide the noninterfering third beam which overlapped the pump and signal beam interaction region with a spot diameter slightly larger ($\sim$3.8 mm diameter at $1/e^2$) than the pump and signal beam diameters. The slightly larger diameter of the He-Ne laser beam ensured good spatial overlap with the grating recording beams and also negated any alignment sensitivity of the He-Ne beam on the gain measurements.

The hybrid cell comprised two windows of 0.1% cerium doped strontium barium niobate (Ce:SBN) with dimensions 20 mm$\times$20 mm$\times$1.3 mm. The crystal c axes were aligned parallel to one of the 20-mm-long edges and the cell was assembled with the crystal axes parallel to each other and oriented parallel to the plane of the incident 532 nm polarization, as shown in Fig. 8. The internal faces were spin coated with a 0.125 wt % solution of Elvamide® (DuPont) nylon multipolymer in methanol followed by unidirectional parallel rubbing orthogonal to the crystal c-axes directions. The combination of this surface treatment with the use of the Ce:SBN windows produces a splayed planar alignment of the liquid-crystal layer [13,14]. The cell was assembled using 10-μm-thick plastic spacers to define the liquid-crystal layer thickness and filled by capillary attraction of the TL205 liquid crystal into the cell void.

As discussed above, the gain contributions from the Ce:SBN and the liquid-crystal layer were separately identified by comparing the cell gain measurements with and without the liquid crystal present. Reference gain measurements were first taken by filling the cell with oil of a similar refractive index to the TL205 liquid crystal (Cargille® type A, $n=1.515$). The gain of the oil filled cell was then measured as a function of the grating spacing both with and without the He-Ne laser present. After disassembly, cleaning, recoating, and reassembly, the cell gain was measured when filled with the liquid crystal, both with and without the He-Ne laser present. The oil-filled cell allowed the exponential gain coefficient of the Ce:SBN substrates to be calculated directly from the net optical gain and the physical path length of the signal beam through the two Ce:SBN windows. The net gain of the liquid-crystal-filled cell was then divided by the relevant oil filled cell gain (with or without the He-Ne) to obtain the liquid-crystal gain as a function of grating spacing. The exponential gain coefficient of the liquid-crystal layer with and without the He-Ne laser present was then determined from the calculated gain and the physical path length through the liquid-crystal layer.

Specific details of the calculation are as follows. Define the following quantities:

G_2^{oil}: total gain through the system with oil-filled cell without the third He-Ne beam;

G_3^{oil}: total gain through the system with oil-filled cell with the third beam;

G_2^{lc}: total gain through the system with liquid-crystal-filled cell without the third beam;

G_3^{lc}: total gain through the system with liquid-crystal-filled cell with the third beam, where "system" here refers to the total system including the cell and the sandwiching photorefractive windows. Suppose the photorefractive windows have total thickness D. Let the exponential gain coefficients in the photorefractive windows be γ_2 and γ_3 in the absence and presence, respectively, of the third beam. Now, when it is filled with oil, the cell plays no part in the optical gain process, and we can write

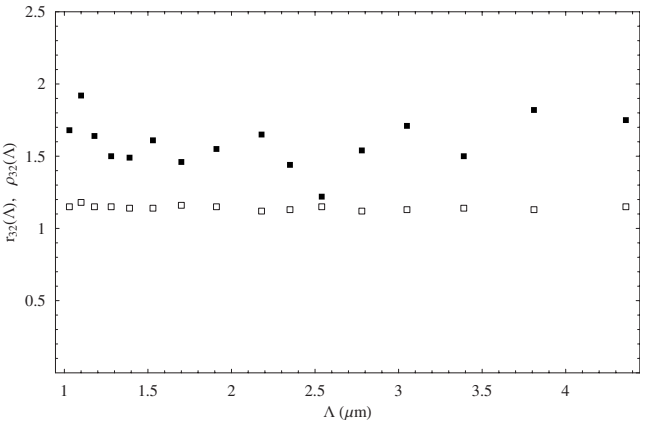

FIG. 9. The quantities $\rho_{32}(\Lambda)$ (squares) $r_{32}(\Lambda)$ (circles), defined in the text. The relation $r_{32}(\Lambda)=\rho_{32}^3(\Lambda)$ is consistent with the theoretical interpretation of Sec. V C. According to this interpretation, the Λ-dependence of the exponential gain coefficient g is explicable in terms of a cubic dependence of the photorefractive space charge.

$$G_2^{oil}=e^{\gamma_2 D}, \quad G_3^{oil}=e^{\gamma_3 D}. \tag{60}$$

The theory of exponential gain coefficients in photorefractive media is well understood [23], and we know that the quantities γ are proportional to the relevant space-charge fields. Then combining the two parts of Eq. (60) yields the following relation:

$$\rho_{32}=\frac{\gamma_2}{\gamma_3}=\frac{\ln G_2^{oil}}{\ln G_3^{oil}}=\frac{|E_{0sc}(q)|}{|E_{0sc}^{(3)}(q)|}, \tag{61}$$

where $E_{0sc}^{(3)}(q)$ is the space-charge field in the bulk photorefractive media as modified by the presence of the third beam.

By analogy with Eq. (60), we can also write

$$G_2^{lc}=e^{\gamma_2 D+gL}, \quad G_3^{lc}=e^{\gamma_3 D+g^{(3)}L}, \tag{62}$$

where the quantity $g^{(3)}$ is the exponential gain coefficient in the liquid crystal in the presence of the third beam. Combining Eqs. (60) and (62) yields

$$r_{32}=\frac{g}{g^{(3)}}=\frac{\ln G_2^{oil}}{\ln G_3^{oil}}\left[\frac{\dfrac{\ln G_2^{lc}}{\ln G_2^{oil}}-1}{\dfrac{\ln G_3^{lc}}{\ln G_3^{oil}}-1}\right], \tag{63}$$

where the quantity r_{32} is itself a function of the grating wave number q or spacing Λ. In Fig. 9 we plot ρ_{32} as a function of grating spacing Λ. We find that in the region over which we measure, $\rho_{32}\approx 1.14\pm 0.01$ with no significant Λ dependence. This therefore gives the ratio of the photorefractive space-charge fields with and without the He-Ne. We also plot in

Fig. 9 the behavior of $r_{32}(\Lambda)$. Here the plot is somewhat noisy, but there is no evident Λ dependence, and we find a best fit of $r_{32}(\Lambda) \approx 1.6 \pm 0.1$.

In general we may suppose that $g^{(3)}$ and g are functions of the photorefractive space-charge fields driving the exponential gain coefficients. Then their ratio r_{32} will be the ratio of these functions. The discussion of Sec. V C suggests that this function is proportional to the cube of the space-charge field, which would imply the relation $r_{32}(\Lambda)=\rho_{32}^3(\Lambda)$. Our measurements are consistent with this prediction, although of course, they do not establish it unambiguously.

VI. DISCUSSION

A. Possible mechanisms for nonlinearity

The key result of this paper is that the exponential gain factor of a splayed liquid-crystal cell sandwiched between two photorefractive windows seems to depend on the product of a beam interference term, a flexoelectricity term, and a space-charge term. The space-charge term depends on the photorefractive electric field in the refractive windows. Our theory replaces a naïve linear dependence on the photorefractive electric field by a cubic dependence.

The evidence for this modification is somewhat indirect but comes from two independent kinds of experiment, and we believe that the result may be regarded as established. On the other hand, the simplest theory (which we have labeled "naïve" in Secs. II–IV) unambiguously predicts an exponential gain factor linear in photorefractive electric field. It is therefore of considerable interest to understand the discrepancy between the naïve theory and experiment. What is the origin of the nonlinear response?

We do not propose in this paper to answer this question definitively, not least because a definitive answer would require further experiments. We can, however, draw some analogies with other work and also make some speculations concerning this particular problem. As long ago as 1976 Prost and Pershan [32], in a classic paper, showed that a grating could be formed using interdigitated electrodes and a homeotropic cell. They too find some nonlinear dependence on the voltage across the interdigitated electrodes. There is clearly some analogy between a voltage caused by interdigitated electrodes and one caused by a leakage of an (optically induced) photorefractive field, and in future work we hope to explore this analogy in greater detail. However at this stage there is no straightforward way of using the results of Prost and Pershan.

We now examine in outline some possible origins for the cubic dependence of the gain on photorefractive field.

1. Pretilt dependence on photorefractive field

We might postulate a nonlinear dependence of the director pretilt angles at the LC cell planes on $E_{0sc}(q)$. This might take the form $\theta_1=\frac{\pi}{180}(1+\alpha E_{0sc}^2)$, $\theta_2=-\frac{\pi}{180}(1+\alpha E_{0sc}^2)$ where α is a fitting parameter. More detailed calculations suggest that such a hypothesis can indeed predict $g_{\max}$ of the right order. However, according to this hypothesis $\Lambda_{\max}$ is still much larger than that observed in experiment and, unlike in experiment, is sensitive to cell thickness.

2. Anchoring energy dependence on photorefractive field

Alternatively, the space-charge field could modify the LC anchoring. The physical idea would be that the space-charge field reorients, for example, the polymer side chains close to the cell substrates. In this case, for example, the coefficient W in Rapini-Papoular surface anchoring term $F_S=\frac{1}{2}W\cos^2(\theta-\theta_{easy})$ would be augmented by a term proportional to $\varepsilon E_{0sc}\cdot E_{0sc}$ due to the space-charge field torque on the polymer chains at the liquid-crystal interface. In this case, one might expect that there will be a change in the easy orientation angle $\theta \propto E_{0sc}^2$. This might in principle lead to a E_{0sc}^3 dependence of the exponential gain coefficient. However, in practice we find that our results for g are very insensitive to W, and any E_{0sc}^3 contribution to the gain will be negligibly small.

3. Inhomogeneous distribution of LC flexoelectric dipoles

The argument of Secs. II–IV uses the standard formula (11) for liquid-crystal flexopolarization. The argument requires that the liquid crystal be chemically uniform throughout the sample. This is a usual assumption in liquid-crystal device modeling, but has not been investigated in any detail. Equivalently, an implicit assumption is that the spatial distribution of the molecular dipoles in the flexoelectric LC be homogeneous. Suppose, however, that the flexoelectric LC is a mixture, in which there exist different moieties with unequal dipoles. In this case, the flexopolarization $\mathbf{P}_f(\boldsymbol{r})$ may depend not only on the director gradient in the point $\boldsymbol{r}$ but also on the concentration of molecules with different dipoles nearby this point.

This effect might be particularly pronounced if such a flexoelectric LC were to be placed in an inhomogeneous electric field. Then molecules with higher dipoles will be attracted toward the region of higher electric field, thereby displacing molecules with smaller dipoles. The consequence would be that the flexoelectric coefficients would exhibit strong spatial dependence. In a real system, there might be many components, and there would also be feedback effects on the director.

We have carried out calculations based on this hypothesis. A more detailed and comprehensive analysis of the effects of LC component separation on optical transmission through liquid-crystal samples will be presented elsewhere [34]. The result is that we can replace the "bare" flexoelectric coefficients occurring in Eq. (11) by "effective" flexoelectric coefficients $e_{ii}=e_{ii}^0(1+\mu q^2|E_{0sc}(q)|^2)$, where μ is a fitting parameter, which is dependent on the thickness of the cell. This modified flexoelectric coefficient would have the effect of bringing the theory more into agreement with the experiment, and we regard this hypothesis as worthy of further more exhaustive study.

4. Inhomogeneous distribution of LC flexoelectric quadrupoles

Flexoelectricity may also be due to permanent molecular quadrupoles in one of the components of the liquid-crystalline mixture. As in the previous example, an inhomogeneous electric field can induce chemical inhomogeneities

in the LC mixture, and this too would replace bare by effective flexoelectric coefficients $e_{ii}=e_{ii}^0(1+\mu q^2|E_{0sc}(q)|^2)$, as above. A related mechanism has been discussed by Schmidtke and Coles [33] in chiral systems. Quantitative estimates suggest that this possibility is feasible, and we also discuss this further elsewhere [34].

B. Conclusions

We have developed a theoretical model to describe the experimentally observed energy gain of the weak signal beam interacting with the strong pump beam in a photorefractive hybrid LC cell. The diffraction grating is written in a flexoelectric nematic layer placed between two inorganic photorefractive windows. The space-charge field induced by interfering light beams in the photorefractive substrates penetrates into the LC layer. Flexoelectric polarization in the LC bulk arises from the interaction between the space-charge electric field and the initial director pretilt at the cell substrates. The flexoelectric polarization writes the diffraction grating in the LC cell and is the main physical mechanism governing the magnitude of the LC layer grating and hence of the two-beam coupling. Experimental data of the gain coefficient in the hybrid cell filled with LC mixture TL 205 show that the magnitude of the director grating is a nonlinear function of the space-charge field.

In this paper we have been able to develop a parameterization which successfully describes most of the experimental results. Our model requires only one fitting parameter at each cell thickness, and the fitting parameter is at best only weakly thickness dependent. The microscopic origin of the nonlinearity is at present not entirely clear. The most hopeful possibility focuses on the fact that the liquid crystal is not a pure system but a mixture. Within this hypothesis, the inhomogeneous photorefractive space-charge field within the liquid crystal induces chemical moiety inhomogeneities, which interact with the flexoelectricity to produce a nonlinear response. The resulting quantitative model is the subject of vigorous current research, and we shall report on this elsewhere.

ACKNOWLEDGMENTS

This work was partially supported by EOARD Grant No. 078001 (V.Y.R. and I.P.P.) and by NATO Grant No. CBP-.NUKR.CLG.981968 "Electro-optics of heterogeneous liquid-crystal systems." We thank Ken Singer, Rolf Petschek, Malgosia Kaczmarek, and Giampaolo D'Alessandro.

[1] L. Solymar, D. J. Webb, and A. Grunnet-Jepsen, *The Physics and Applications of Photorefractive Materials* (Clarendon Press, Oxford, 1996).
[2] G. Cook, C. J. Finnan, and D. C. Jones, Appl. Phys. B: Lasers Opt. **68**, 911 (1999).
[3] G. P. Wiederrecht, B. A. Yoon, and M. R. Wasielewski, Science **270**, 1794 (1995).
[4] I. C. Khoo, B. D. Guenther, M. V. Wood, P. Chen, and M.-Y. Shih, Opt. Lett. **22**, 1229 (1997).
[5] H. Ono and N. Kawatsuki, J. Appl. Phys. **85**, 2482 (1999).
[6] E. V. Rudenko and A. V. Sukhov, JETP Lett. **59**, 142 (1994).
[7] E. V. Rudenko and A. V. Sukhov, Sov. Phys. JETP **78**, 875 (1994).
[8] I. C. Khoo, H. Li, and Y. Liang, Opt. Lett. **19**, 1723 (1994).
[9] A. Brignon, I. Bongrand, B. Loiseaux, and J. P. Huignard, Opt. Lett. **22**, 1855 (1997).
[10] F. Kajzar, S. Bartkiewicz, and A. Miniewicz, Appl. Phys. Lett. **74**, 2924 (1999).
[11] S. Bartkiewicz, K. Matczyszyn, A. Miniewicz, and F. Kajzar, Opt. Commun. **187**, 257 (2001).
[12] G. Cook, C. A. Wyres, M. J. Deer, and D. C. Jones, Proc. SPIE **5213**, 63 (2003).
[13] G. Cook, J. L. Carns, M. A. Saleh, and D. R. Evans, Mol. Cryst. Liq. Cryst. **453**, 141 (2006).
[14] R. L. Sutherland, G. Cook, and D. R. Evans, Opt. Express **14**, 5365 (2006).
[15] D. R. Evans and G. Cook, J. Nonlinear Opt. Phys. Mater. **16**, 271 (2007).
[16] G. Cook, A. V. Glushchenko, V. Reshetnyak, A. T. Griffith, M. A. Saleh, and D. R. Evans, Opt. Express **16**, 4015 (2008).
[17] G. Cook, E. Beckel, V. Reshetnyak, M. A. Saleh, and D. R. Evans, in *Controlling Light with Light: Photorefractive Effects, Photosensitivity, Fiber Gratings, Photonic Materials and More: OSA Technical Digest (CD) [Photorefractive Effects, Photosensitivity, Fiber Gratings, Photonic Materials and More (PR) Squaw Creek, California October 2007]* (Optical Society of America, Washington, DC, 2007).
[18] N. V. Tabiryan and C. Umeton, J. Opt. Soc. Am. B **15**, 1912 (1998).
[19] D. C. Jones and G. Cook, Opt. Commun. **232**, 399 (2004).
[20] M. Kaczmarek, A. Dyadyusha, O. Buchnev, Yu. Reznikov, and V. Yu Reshetnyak, Nonlinear Opt., Quantum Opt. **35**, 217 (2006).
[21] O. Buchnev, A. Dyadyusha, M. Kaczmarek, V. Yu Reshetnyak, and Y. Reznikov, J. Opt. Soc. Am. B **24**, 1512 (2007).
[22] V. O. Kubytskyi, V. Y. Reshetnyak, T. J. Sluckin, and S. J. Cox, Phys. Rev. E **79**, 011703 (2009).
[23] P. Yeh, *Introduction to Photorefractive Nonlinear Optics* (Wiley, New York, 1993).
[24] P. G. de Gennes and J. Prost, *The Physics of Liquid Crystals*, 2nd ed. (Clarendon Press, Oxford, 1993), p. 136.
[25] See also S. T. Lagerwall, *Ferroelectric and Antiferroelectric Liquid Crystals* (Wiley, Weinheim, 1999), Chap. 4; http://www3.interscience.wiley.com/cgi-bin/bookhome/117871070/, for a more comprehensive discussion of liquid-crystal flexoelectricity.
[26] E. G. Edwards, C. V. Brown, E. E. Kriezis, and S. J. Elston, Mol. Cryst. Liq. Cryst. **400**, 13 (2003).
[27] D. L. Cheung, S. J. Clark, and M. R. Wilson, J. Chem. Phys. **121**, 9131 (2004).
[28] J. Stelzer, R. Berardi, and C. Zannoni, Chem. Phys. Lett. **299**, 9 (1999).

[29] M. P. Allen and A. J. Masters, J. Mater. Chem. **11**, 2678 (2001).
[30] H. Kogelnik, Bell Syst. Tech. J. **48**, 2909 (1969).
[31] W. R. Klein and B. D. Cook, IEEE Trans. Sonics Ultrason. **SU-14**, 123 (1967).
[32] J. Prost and P. S. Pershan, J. Appl. Phys. **47**, 2298 (1976).
[33] J. Schmidtke and H. J. Coles, Phys. Rev. E **80**, 011702 (2009).
[34] I. P. Pinkevych *et al.* (unpublished).